SURFACE TENSION LOCKUP IN THE IMAGE NUTATION DAMPER – ANOMALY AND RECOVERY

Carl Hubert
Hubert Astronautics, Inc.

Daniel Swanson
Lockheed Martin Space Systems

ABSTRACT

Early telemetry from the spin-stabilized IMAGE spacecraft indicated that the vehicle's initial nutation was not decaying. This behavior was especially puzzling because the spacecraft's passive nutation damper behaved as expected while IMAGE was attached to the spinning upper stage. The lack of damping was also puzzling because the damper was a tubular ring partially filled with liquid mercury; a simple, reliable device with a long flight history. In a partially-filled ring damper, the excess kinetic energy associated with nutation is dissipated by fluid viscosity when inertial forces cause the liquid to move through the tube. However, post-launch analysis indicated that the IMAGE damper liquid was immobilized by surface tension. This was an unanticipated consequence of the vehicle's low spin rate. When it became apparent that passive damping did not work, a ground-commanded open-loop damper was developed using the spacecraft's magnetic torquer and onboard logic that was intended for ground test of the torquer. This work-around successfully resolved the IMAGE nutation damping problem.

INTRODUCTION

The mission of IMAGE (Imager for Magnetopause to Aurora Global Exploration) is to obtain global images of the major plasma regions and boundaries in the Earth's inner magnetosphere, and to study their dynamic response to the flow of charged particles from the sun. The payload consists of two ultraviolet imagers, three neutral atom imagers, and a radio sounding imager (RPI – Radio Plasma Imager). In the fully-deployed mission configuration, the RPI has two 10-meter antennas that extend parallel to the spin axis, and four 250-meter radial wire antennas (Fig. 1). The RPI antennas were stowed during launch and during the early stages of mission operations that are the focus of this paper. The core of the IMAGE spacecraft (minus the RPI antennas and the helix antenna) is 2.25 meters in diameter and 1.52 meters high. The vehicle's attitude and spin rate (nominally 0.5 rpm during mission operations) are controlled by a single magnetic torque rod, with attitude information being provided by a sun sensor, a star tracker, and a 3-axis magnetometer. IMAGE also has a ring nutation damper that was designed to attenuate nutation caused by launch vehicle separation and spacecraft maneuvers.

As shown in Fig. 2, the damper is simply a round tube that is bent into a closed, circular ring and half-filled with mercury. In this type of device, kinetic energy is dissipated when nutational motion causes the liquid to move through the tube. On IMAGE, the tubular ring is centered on and perpendicular to the vehicle's nominal spin axis. It is also displaced as far as possible from the vehicle's center of mass (see parameter h in Fig. 2). Dampers of this type have a long history, with the mercury ring on the 1958 Pioneer 1 lunar probe being the first nutation damper to be flown in space [1]. Since that first flight, numerous papers and reports have been written on the subject [2–13]. However, despite the inherent reliability of this simple device, early telemetry indicated that IMAGE's damper didn't work after separation from the launch vehicle.

IMAGE was launched on a Delta II with a spinning upper stage. During third stage operations, the combined vehicle (spacecraft plus third stage) spun about its minimum moment of inertia axis. In this type of configuration, energy dissipation causes nutation to grow. During third stage operations, the only significant energy dissipation

mechanism was the spacecraft's nutation damper. Pre-flight analysis of the damper indicated that there would be negligible nutation growth during the brief coast between the stage 2/3 separation and third stage ignition. Specifically, nutation was expected to grow exponentially with a time constant ≥3,300 sec. The actual flight performance matched this expectation, with no detectable growth from the initial 0.03 deg. nutation. Although a low signal-to-noise ratio made it impossible to determine an accurate flight divergent time constant, it is clear that if there was any growth, the time constant must have been >1,000 sec. Although this does not confirm the pre-flight prediction, it is consistent with it.

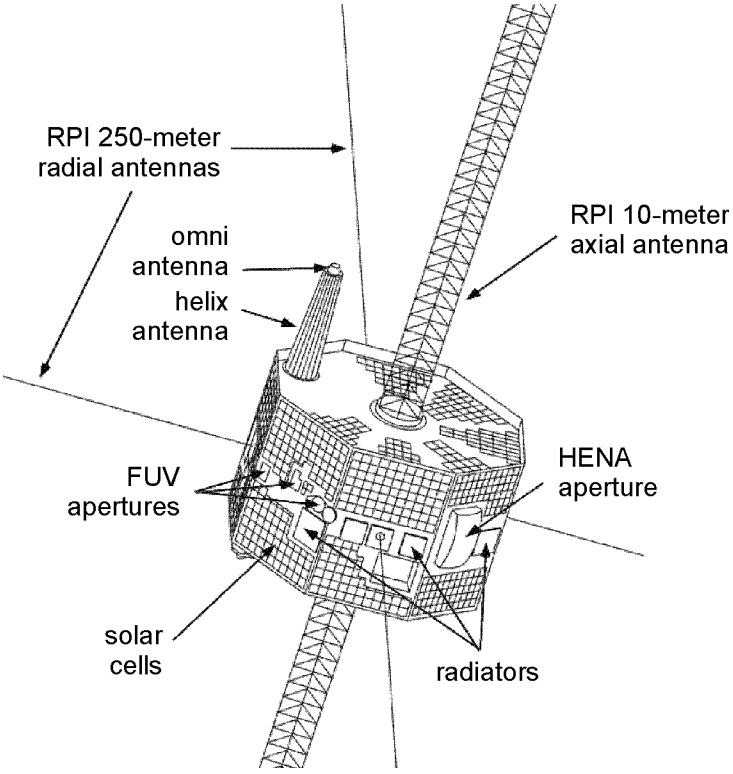

Figure 1. IMAGE in its fully-deployed mission configuration

Unlike the pre-burn case, the post-burn configuration was expected to experience rapid nutation growth with a consequent vigorous activity by the third stage's active nutation damper. Once again, flight performance was consistent with expectation, with Boeing reporting that the IMAGE flight involved more nutation control pulsing than any other Delta II launch to date. The rate of nutation growth between thruster pulses indicates that the damper's mean energy dissipation rate was approximately 0.14 watts. This compares favorably with the expected value of approximately 0.18 watts, and from this one can conclude that the damper was intact during third stage operations.

Although the nutation damper performed as expected while the third stage was attached, the story was quite different after the yo-yo despin and separation. At first contact, IMAGE was observed to be spinning at 3.1 rpm

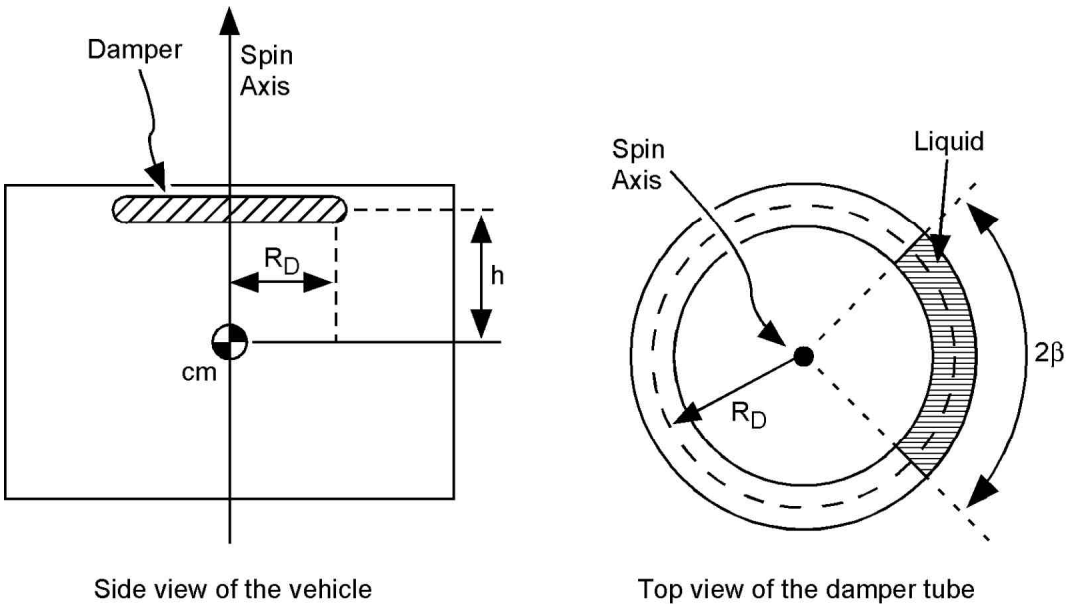

Figure 2. The partially-filled ring damper (not to scale)

with a 3.5 deg. nutation. Although the spin rate and nutation amplitude were within expected limits, there was virtually no nutation damping. This was especially surprising because the damper was clearly functioning less than an hour earlier when the third stage was attached. After an investigation ruled out the possibility of nutation pumping by a thermoelastic effect, it was concluded that some mechanism prevented the nutation damper from functioning under the post-separation conditions. A mercury leak was considered unlikely because it would have required a sudden, catastrophic failure and the spacecraft was clearly healthy. It was finally determined that at IMAGE's low post-separation spin rate, the mercury in the damper tube was immobilized by surface tension. This paper discusses the damper's anomalous behavior and the method that was used to overcome the problem.

SURFACE TENSION AND THE FLOW OF MERCURY THROUGH A TUBE

Of the researchers who have worked on ring dampers, only Hinada and Inatani [10] addressed surface tension as a factor that can affect damper performance, and then only as an additional drag that modifies the damping rate. Hong [14] appears to be the only one to have addressed surface tension lockup as a limiting factor on the capability of liquid-filled dampers. Hong's focus was on the residual nutation angle for fluid dampers with endpots. Although ring dampers were not included in that study, Ref. 14 clearly indicates that a liquid free surface can be immobilized by surface tension at low spin rates, and that once the liquid is immobilized it no longer damps nutation.

A liquid surface that is in contact with an atmosphere has an apparent "skin" that can support small loads and that acts very much like a membrane under tension. This behavior, which is commonly referred to as "surface tension," results from cohesive intermolecular forces. A liquid in contact with a solid surface will adhere to that surface. Depending on the liquid and solid, the adhesive force can be greater than or less than the cohesive force. If the adhesive force exceeds the cohesive force, the liquid tends to spread outward and is said to "wet" the surface. If the cohesive force exceeds the adhesive force, the liquid contracts inward and is said to be "non-wetting." It is important recognize, however, that "non-wetting" does not mean "non-adhesive." For both wetting and non-wetting liquids there is a surface tension force between the liquid and solid at the three phase line where liquid, gas, and solid all meet. This force is perpendicular to the three phase line and is parallel to the liquid's free surface.

Figure 3 illustrates the interaction of a liquid free surface with the walls of a narrow tube. The upper part of the figure shows a tube that contains a wetting liquid and the lower part shows a tube that contains a non-wetting liquid. In both cases, surface tension applies a force, F_S, to the wall and the wall applies an equal and opposite force, F_W, to the liquid. These forces are applied at an angle, θ, relative to the tube wall. This contact angle is a function of the materials (liquid, solid, and gas) and of physical parameters such as temperature and pressure. Wetting liquids have contact angles less than 90 deg. and non-wetting liquids have contact angles greater than 90 deg. Mercury's nominal contact angle with stainless steel is approximately 133 deg.

Although the term "surface tension" is used broadly to refer to the phenomena under consideration here, the term also applies more specifically to the force at the surface of a liquid. This parameter has the units of force per unit length. To determine the total force between the liquid surface and a tube wall, one must integrate the surface tension over the three phase line. For a circular tube, the net force is given by:

$$F_{NET} = 2 \pi R_T \sigma \cos(\theta) \tag{1}$$

where σ is the surface tension and R_T is the tube's inside radius. Note that this force is parallel to the tube's long axis. Note also that the sign of the force depends on whether the liquid is wetting or non-wetting. For a wetting liquid, surface tension causes the liquid to advance down the tube unless it is restrained by a counteracting force. A non-wetting liquid tends to retreat.

As a liquid slug moves down a tube in response to inertial forces, the contact angle increases on the advancing end and decreases on the receding end. As discussed in Ref. 10, the difference in contact angle between the advancing and receding ends means that the net surface tension forces are unequal at the two ends. The resulting retarding force is similar to Coulomb friction because it is essentially independent of the velocity of the liquid slug through the tube. This, in turn, means that there is a "stiction" effect that can halt the liquid if its velocity becomes

small enough. Furthermore, it means that if the inertial forces are small enough, the liquid cannot be made to move. This is true whether the liquid is wetting or non-wetting.

Contact angle differences can also exist in the static case if there is a pressure difference between the two ends. This behavior is illustrated in Fig. 4, which denotes the advancing and receding contact angles with the symbols θ_A and θ_R. The net surface tension force on the liquid slug is given by the following equation:

$$F_S = 2 \pi R_T \sigma [\cos(\theta_R) - \cos(\theta_A)] \qquad (2)$$

To start the liquid slug moving, the inertial force must exceed the surface tension force for the greatest possible difference between θ_A and θ_R. Test results reported in Ref. 15 indicate a static contact angle hysteresis for mercury on stainless steel of 124 to 146 deg. at 25°C in a nitrogen atmosphere. Using the contact angles from Ref. 15 along with IMAGE's tube radius of 0.55 cm and mercury's nominal surface tension of 0.475 N/m, we see that a minimum force of 0.0044 N (0.0010 lb) is needed to get the mercury slug moving. Although this force is small, it is close to the peak inertial force on the IMAGE liquid slug after separation from the third stage.

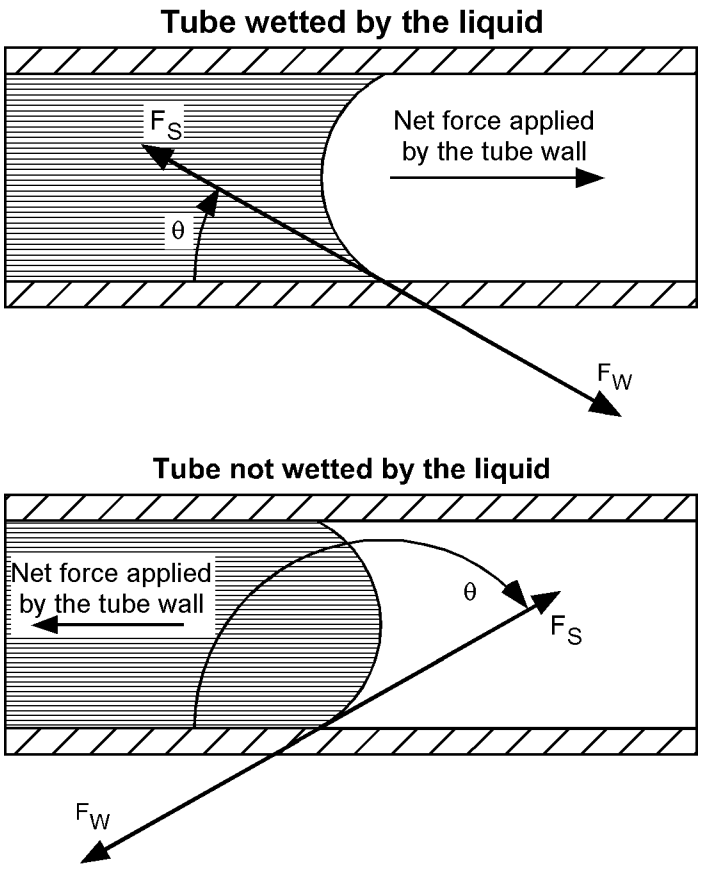

Figure 3. Contact angle and net force for wetting and non-wetting liquids in a tube

The contact angle hysteresis reported in Ref. 15 was measured using triple-distilled mercury on a stainless steel plate that was polished to a mirror finish. These conditions do not exist in a real damper. Roughness of the solid surface can increase the hysteresis and thereby increase the force required to start the mercury slug moving. Contaminants on the tube wall (such as welding byproducts) may alter the contact angles; as can contamination of the mercury surface. Contamination of the mercury surface also alters the surface tension. Finally, the IMAGE damper contained a helium atmosphere rather than the nitrogen atmosphere that was used for the tests reported in Ref. 15. For all of these reasons, calculations with Eqn. 2 must be considered to be approximations.

SURFACE TENSION AND CENTRIFUGAL FORCE

Although liquid mobility within a ring damper depends on the component of the inertial force that is parallel to the tube's long axis, the ratio of centrifugal force to surface tension force is a simple indicator of whether there is a

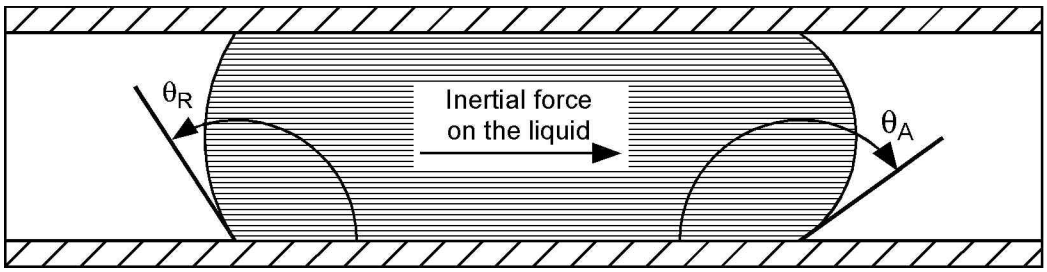

Figure 4. Advancing and receding contact angles for a stationary mercury slug subject to inertial force

potential lockup problem. This ratio, called the Bond number, is given by the following expression:

$$N_B = \rho R_D R_T^2 \Omega^2 / \sigma \quad (3)$$

where ρ is the fluid density, R_D is the distance from the center of the damper to the tube centerline (see Fig. 2), and Ω is the vehicle's spin rate. Surface tension can usually be ignored if $N_B > 100$, has a minor effect if $10 < N_B < 100$, has a potentially large effect if $1 < N_B < 10$, and is dominant if $N_B < 1$. The Bond number's effect on the liquid distribution is illustrated in Fig. 5, which assumes the ideal case of a perfectly aligned damper on a balanced spacecraft with no nutation. With a high Bond number, centrifugal force spreads the liquid uniformly around the tube. If the Bond number is low, the liquid collects into one or more continuous slugs that completely fill the tube diameter. Under this condition, surface-tension lockup is possible at a non-trivial nutation angle.

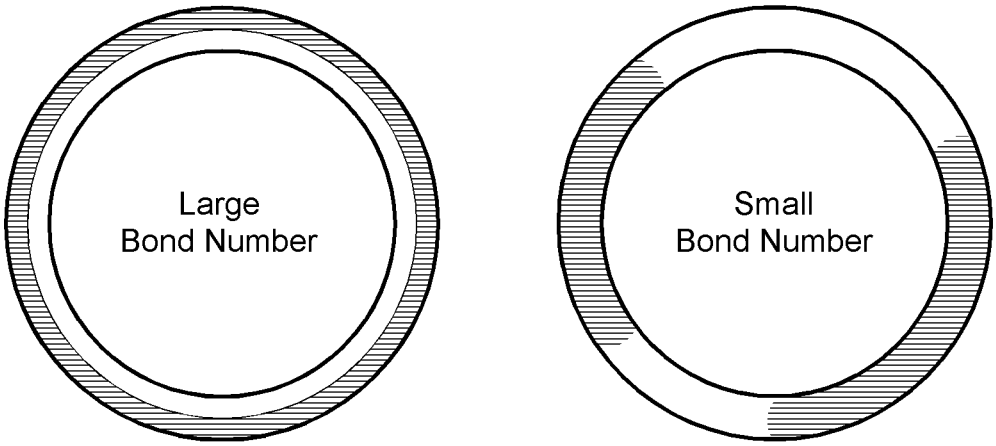

Figure 5. The effect of Bond number on liquid distribution

When IMAGE was on the third stage and spinning at 49 rpm, the centrifugal Bond number was 6.7, which indicates little potential for surface tension lockup. At the 3.1 rpm post-separation rate, however, the Bond number dropped to 0.027, a clear indication that the damper would stop functioning at a non-trivial nutation angle. Finally, at the 0.5 rpm operational spin rate, IMAGE's centrifugal Bond number was only 0.00070. This is an unambiguous indicator that the nutation damper will not work at that spin rate.

SURFACE TENSION LOCKUP IN A PARTIALLY FILLED DAMPER

As discussed above, a minimum inertial force is needed to start a liquid slug moving against the restraining effect of surface tension. For a ring damper on a nutating spacecraft, a stationary liquid slug is subject to a cyclic force parallel to the tube's centerline. As shown in the Appendix, the cyclic nutational force on a slug with a half angle β (see Fig. 2) has an amplitude that is given by

$$F_N = 2 \pi h \gamma^2 \rho \Phi \Omega^2 \sin(\beta) R_D R_T^2 \quad (4)$$

where γ is the vehicle's inertia ratio, Φ is the nutation angle, and h is the displacement of the damper from the center of mass (Fig. 2). This equation assumes that the spacecraft is inertially symmetric (i.e., the vehicle is inertially equivalent to a homogeneous right circular cylinder). Because IMAGE was nearly symmetric, this assumption has only a small effect on the accuracy of the results. The derivation of Eqn. 4 also involved the assumption that the nutation angle is small (less than about 15 deg.). For the liquid slug to be able to move, we must have

$$F_N > F_S \quad (5)$$

From Equations 2, 4, and 5 it is easy to see that liquid slug motion requires that

$$\Phi > \frac{\sigma[\cos(\theta_R) - \cos(\theta_A)]}{h\gamma^2\rho\Omega^2 R_D R_T \sin(\beta)} \tag{6}$$

It is essential to recognize that the slug may not move if this inequality is barely satisfied because F_N represents the peak of a cyclic force; not a continuous force. The free surfaces at the two ends of the slug act somewhat like springs. The slug center of mass must be displaced a short distance before these "springs" are stretched to their limits and the slug actually breaks free. In other words, it takes a finite amount of time for the inertial force to displace the liquid slug to the point where the advancing and retreating contact angles reach their limits. If the time required to reach these limits is shorter than the time that the cyclic force satisfies Eqn. 5, then surface tension will prevail and the slug will be immobilized.

A problem with applying Eqn. 6 is the uncertainty in the half angle, β. For a half-filled damper with the liquid collected into a single contiguous slug, we have $\beta = 90$ deg. However, the liquid can be fragmented into a collection of smaller slugs of indeterminate size. This fragmentation increases the nutation angle needed to free the largest slug. Yet another problem is the uncertainty in the tube's surface roughness and in the nature, amount, and effect of any contaminants. Because of these uncertainties, it is possible that calculations using Eqn. 6 could be in error by as much as a factor of two. It must also be noted that Eqn. 6 was derived with the assumption that the three phase line forms a circle perpendicular to the tube's centerline. This assumption becomes increasingly invalid as the Bond number increases. Centrifugal force causes the true three phase line to be elliptical and tilted relative to the tube centerline. For this reason, Eqn. 6 is probably inaccurate when the Bond Number is much greater than 2.

ANALYSIS OF THE IMAGE RING DAMPER

Table 1 lists key parameter values for the IMAGE nutation damper. These parameters were used to calculate the nutation angle at which the liquid slug would break free at various points in the mission, and the results are presented in Table 2. The "release angles" in Table 2 were calculated using Eqn. 6 for a 180 deg. slug ($\beta = 90$ deg.). As indicated previously, this assumption plus other uncertainties means that the calculated angles could be in error by as much as a factor of 2. As Table 2 suggests, it is possible that the that lack of observable nutation growth before the third stage burn was due to surface tension lockup. However, the high Bond number means that the calculated slug release angle may be inaccurate. Furthermore, even if the nutation damper did perform according to preflight calculations, there should have been no observable nutation growth. One can thus draw no conclusions from that portion of the mission.

The rapid nutation growth that followed IMAGE's third stage burn was as expected. This is consistent with the calculated slug release angle being two orders of magnitude smaller than the observed nutation angle. For the two tabulated cases that followed IMAGE's separation from the third stage, the calculated slug release angles were slightly lower than the nutation angles at which no damping was observed. As previously indicated, however, there

Table 1. Nutation Damper Parameters

Tube inside diameter	1.09 cm
Hoop radius (to tube centerline)	30.0 cm
Distance from vehicle cm – third stage pre-burn coast	166 cm
Distance from vehicle cm – third stage post-burn coast	103 cm
Distance from vehicle cm – after separation from third stage	62.5 cm
Fill fraction	0.50
Mercury mass	1.19 kg
Mercury density @ 25°C	13,550 kg / m^3
Mercury surface tension in a helium atmosphere @ 25°C	0.475 N / m
Mercury contact angle hysteresis against stainless steel @ 25°C	124–146 deg.

Table 2. Damper Performance vs. Expectation

Configuration	Spin Rate (rpm)	Bond Number	Nutation (deg.) Flight Angle	Nutation (deg.) Release Angle*	Observed Nutation Behavior
1. With third stage (pre-burn); $\gamma = 0.442$	48.6	6.7	0.03	0.038†	No growth, as expected from pre-flight analysis
2. With third stage (post-burn); $\gamma = 0.682$	49.2	6.7	2.0	0.025†	Growth rate close to pre-flight predictions
3. After separation from third stage; $\gamma = 1.445$	3.09	0.027	3.5	2.4	No nutation damping
4. After separation from third stage; $\gamma = 1.445$	2.05	0.012	7.0	5.5	No nutation damping

* Calculated using Eqn. 6. Assumes that the liquid forms a single continuous slug and that the tube has no surface roughness or contamination. The actual slug release angles could differ by a factor of two.

† Value is of uncertain accuracy because the Bond number is greater than 2.

is probably a factor of 2 uncertainty in the calculated release angles. The flight nutation angles are well within this uncertainty. It is thus reasonably safe to conclude that the lack of nutation damping can be attributed to surface tension lockup.

GROUND-COMMANDED MAGNETIC NUTATION DAMPER

During the design phase of IMAGE, the possibility of a failed nutation damper was considered in the failure modes and effects analysis. That analysis concluded that if the nutation damper failed, it was possible to damp nutation actively using the magnetic torque rod. However, because of budget and schedule constraints, no effort was made to flesh out the details. If active damping became necessary, it was clear that the spacecraft would be in a safe state for however long it took to work out a procedure.

By the third day after launch it was obvious that the nutation damper was ineffective, and work began on a ground-in-the-loop procedure to damp nutation using the torque rod. Even with an initial false start (described below), the procedure was developed and operational within six days. At the heart of this procedure is a new flight-software macro which activates the torque rod via a mode that was intended for manual control of the rod during ground test. Each time the new macro is activated, it toggles the torque rod polarity 20 times synchronized with the nutation. The start time of the toggle sequence and the duration of each toggle is determined in real-time by the IMAGE Flight Operations Team (FOT) and uplinked to the spacecraft. This section provides the mathematical background for the procedure and the next section provides flight results.

In a spin balance procedure executed at the end of spacecraft integration, the spacecraft mass properties were trimmed using balance weights to align the major principal inertia axis with the spacecraft's geometric Z axis, which is the intended spin axis. The clocking of the minor and intermediate principal axes relative to the geometric X and Y axes is not relevant, so all angles in the spin plane are referenced to the spacecraft geometric XY axes.

For a nutating rigid body spinning about its major principal axis, the angular momentum vector **H** projected onto the body reference frame's XY plane moves in a prograde direction as shown in Fig. 6. To actively damp the nutation, an external torque must be applied to the body to drive the momentum vector toward the origin of the XY plane. The only active control element on IMAGE is the 790 Am^2 magnetic torque rod mounted in the spacecraft XY plane, oriented as shown in Fig. 7. At the time of the nutation damper anomaly, the only attitude sensors

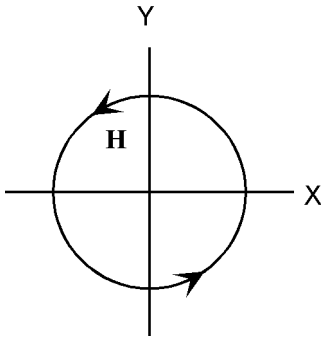

Figure 6. Motion of the angular momentum vector in the XY plane

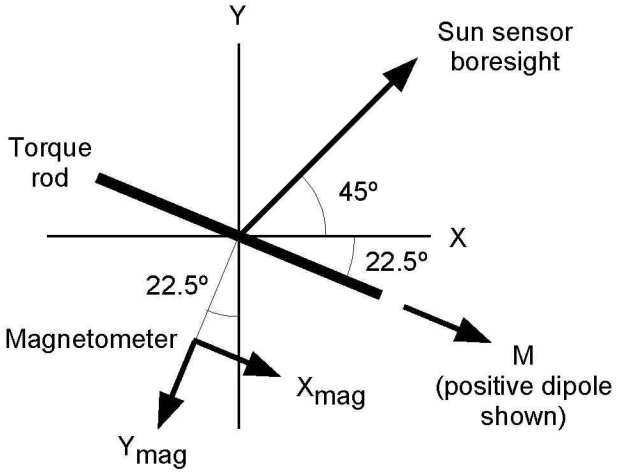

Figure 7. IMAGE component orientations

available were the sun sensor and the 3-axis magnetometer; the spin rate was too high to use the star tracker. The orientation of the sun sensor and magnetometer are shown in Fig. 7.

The dipole **M** generated by the torque rod can be expressed in the spacecraft reference frame as

$$\mathbf{M} = pM \begin{bmatrix} \cos\alpha \\ \sin\alpha \\ 0 \end{bmatrix} \tag{7}$$

where M is the dipole magnitude, α is the torque rod clock angle (-22.5°), and p is the torque rod polarity (+1 for positive, -1 for negative). The spacecraft controls the dipole magnitude and polarity by setting the magnitude and direction of electrical current flowing through the rod windings.

The magnitude and orientation of the Earth's magnetic field at the spacecraft vary with the orbital position of the spacecraft and the rotation of the Earth. Both change slowly relative to the spin rate of the spacecraft. For this analysis it is thus assumed that the field is constant within a spin period, with an in-plane component B_{XY} and an axial component B_Z. In the spacecraft reference frame the in-plane component varies sinusoidally at the spin rate, while the axial component remains constant:

$$\mathbf{B} = \begin{bmatrix} B_{XY}\cos\varphi \\ -B_{XY}\sin\varphi \\ B_Z \end{bmatrix} \tag{8}$$

where **B** is the local magnetic field expressed in the spacecraft reference frame and φ is the spacecraft rotation angle. This angle is arbitrarily set to zero at the instant that the X-component of the magnetic field is at a maximum. Based on these definitions, the torque applied to the spacecraft by the torque rod is

$$\mathbf{T} = \mathbf{M} \times \mathbf{B} = pM \begin{bmatrix} B_Z \sin\alpha \\ -B_Z \cos\alpha \\ -B_{XY}\sin(\alpha + \varphi) \end{bmatrix} \tag{9}$$

The in-plane (X and Y) components of **T** affect nutation, and we will concentrate on these below. The axial (Z) component affects only spin rate. For IMAGE it was more important to control nutation than to maintain a particular spin rate. Hence, the axial component of the torque vector is ignored. As stated above, we assume that

the axial component of the magnetic field is constant within a spin period, and in particular that it does not change sign. Under this assumption, the orientation of the in-plane component of the torque, $\mathbf{T}_{XY}$, is fixed in the spacecraft body frame, and the torque rod polarity p determines whether it points in a positive or a negative direction:

$$\mathbf{T}_{XY} = pMB_Z \begin{bmatrix} \sin\alpha \\ -\cos\alpha \end{bmatrix} \qquad (10)$$

If we know (or can predict) the sign of B_Z, then we can select the torque rod polarity that will produce torque in the desired direction, as shown in Fig. 8. Predicting the sign of B_Z is simple because we know the Earth's magnetic field, IMAGE's orbital position, and the spin axis orientation at any specified time. During IMAGE operations, predicts of B_Z were provided to the FOT by the Flight Dynamics Analysis Branch of the NASA Goddard Spaceflight Center.

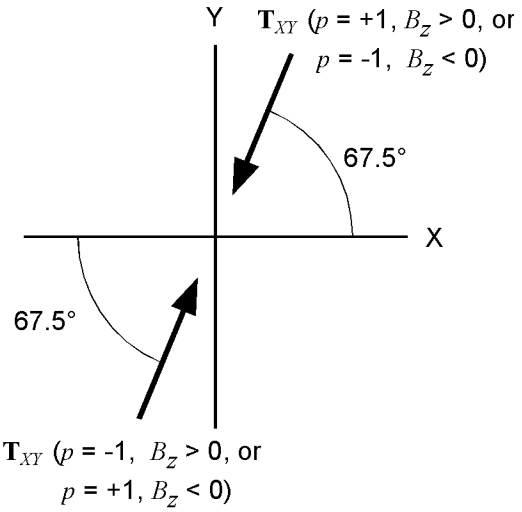

Figure 8. In-plane component of torque produced by the magnetic torque rod

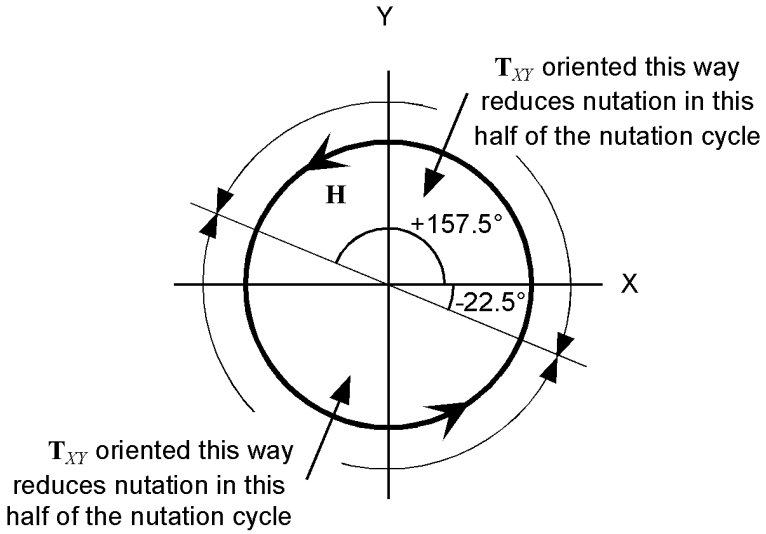

Figure 9. Direction of torque required to reduce nutation

Figure 9 shows that the desired torque direction depends on where in the nutation cycle the torque is applied. The torque must be oriented to drive the projection of the momentum vector toward the origin of the XY plane. For half the nutation cycle, positive torque is needed; for the other half, negative is required. To achieve this, the polarity must be toggled twice per nutation period, once when the nutation phase crosses -22.5°, and again when the phase crosses +157.5°. Unfortunately, the IMAGE flight software contains no logic to distinguish when the nutation phase crosses these transition points. Thus, the only option was to use the downlink telemetry to predict when the transitions would occur, and then to manually toggle the polarity at these predicted times. Predictions were based on sun angle measurements. Once each spin period, as the sun passes through the plane defined by the sun sensor boresight and the spin axis, the sun sensor outputs a measurement of the angle from the spacecraft XY-plane to the sun line (Fig. 10). Because the nutation frequency differs from the spin frequency, each sun angle measurement occurs at a different nutation phase angle, resulting in a slightly different sun angle reading. A series of consecutive sun angle measurements occurs within a band defined by the amplitude of the nutation (Fig. 11). The nutation angle is one-half the width of the band.

Either the maximum or the minimum sun angle measurement within the band can be used as a nutation phase reference. The sun sensor boresight points at +45° in the XY-plane. Both the sun vector and the angular momentum vector are fixed in inertial space. Figure 12 shows the position of the angular momentum vector and the sun vector in the body frame at two different times – at a nutation phase angles of +45° and -135°. The minimum sun angle measurement occurs at +45°, and the maximum occurs at -135°. Along with each sun angle measurement the

telemetry includes the spacecraft clock time at which the measurement was made. This enabled the FOT to determine in real-time the spacecraft clock time at which the nutation phase was +45° by watching for a sun angle minimum and recording the corresponding clock time.

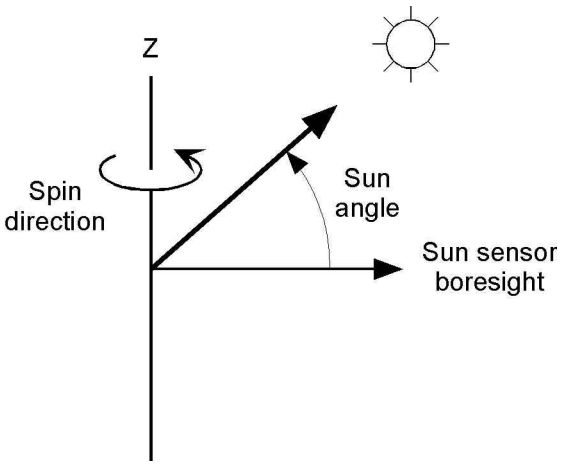

Figure 10. Sun sensor angle measurement

Sun angle measurements were also used to estimate the spacecraft nutation period. To get from one sun angle maximum to the next requires both an integer number of spin periods (because the sun angle is measured once per spin) and an integer number of nutation periods (because the maximum occurs at only one place within the nutation cycle). The prelaunch prediction of the spacecraft mass properties was used for an initial estimate of the nutation period. This estimate was the starting point to find the ratio of the nutation period to the spin period that best fit the time observed between consecutive sun angle maxima. To minimize quantization errors, the data set used for this fit extended over multiple consecutive sun angle maxima (one to two hours of consecutive data).

The ground-in-the-loop nutation damping procedure is as follows:

1. Estimate the nutation period τ using an hour or two of sun angle measurements.

2. Predict the sign of the axial component of the magnetic field, B_Z, using orbital predicts and spin axis attitude. Double-check this predict against the axial component measured by the magnetometer.

3. Monitor the real-time sun angle measurements. Watch for a sun angle measurement close to the minimum of the sun angle band. Record the spacecraft clock time of this minimum. This is the reference sun angle measurement time *RefClock*.

4. Calculate the spacecraft clock time to start toggling the torque rod. This time must be an integer number of nutation periods after the minimum sun angle, plus the time for the nutation phase to rotate from the sun angle minimum at +45° to the torque rod transition phase angle at +157.5°:

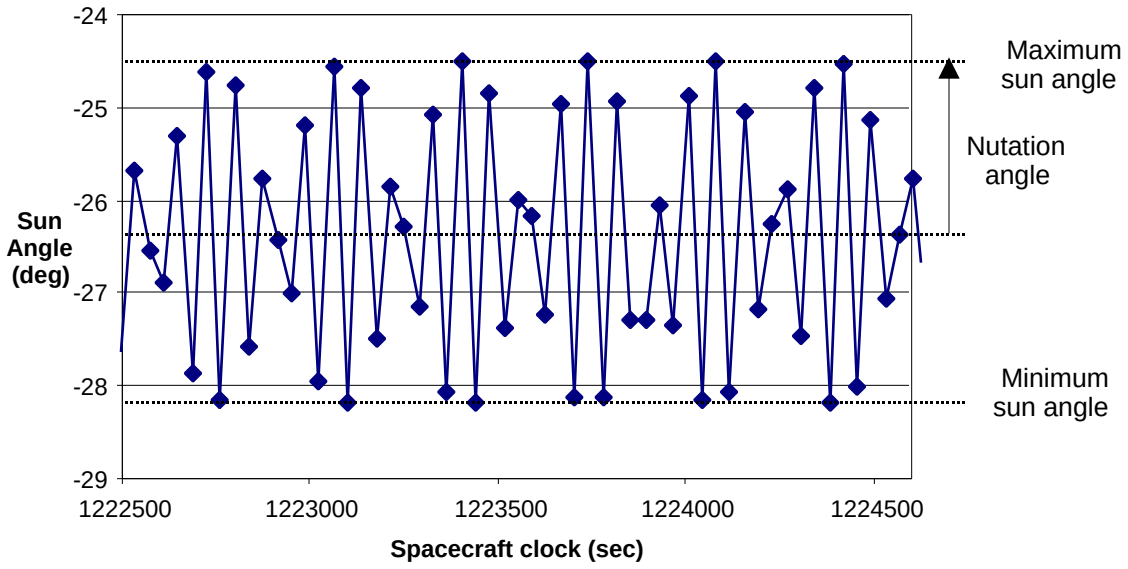

Figure 11. Typical sun sensor output during nutation

$$StartClock = RefClock + k\tau + \left(\frac{112.5^\circ}{360^\circ}\right)\tau \qquad (11)$$

where k is an integer selected such that *StartClock* is about 10 minutes after the time of the reference sun angle measurement. 10 minutes allows sufficient time for the FOT to generate and uplink the flight software macro defined in Step 5.

5. Prepare and uplink a flight software macro to flip the torque rod polarity every $\tau/2$ seconds starting at spacecraft clock time *StartClock*, using the maximum commandable torque rod magnitude. If B_Z is positive, the first torque rod polarity must be negative; if B_Z is negative, the first polarity must be positive. Execute 10 total positive/negative cycles (20 state changes), and then turn the torque rod off.

6. Monitor execution of the macro. Verify that the nutation angle decreases.

The procedure was limited to 10 cycles to minimize the effect of timing errors. An error in the estimate of the nutation period will cause torque rod toggles to deviate further and further from the desired nutation phase angle. For deviations less than 90°, this would reduce the efficiency of the nutation damping, since for part of the nutation period the torque would be applied in the wrong direction. For deviations greater than 90°, the procedure would actually increase nutation rather than reduce it. Hence getting the phasing of the torque rod toggles correct is critical, as will be seen in the next section.

MAGNETIC DAMPER FLIGHT PERFORMANCE

The first attempt to use the magnetic damping procedure was on March 31, 2000, six days after launch (nut #1 on Fig. 13). Although the control logic was very effective at changing nutation, the change was unfortunately in the WRONG direction. A subsequent review of the math model showed a sign error in the correlation of the sun angle measurement to the nutation phase. This error caused the damping torque to be applied 180º out of phase. On April 3 the procedure was repeated with the sign error corrected. This produced the desired damping (nut #2 on Fig. 13). The magnitude of the nutation change is smaller on this and subsequent damping maneuvers because as an additional measure of safety the procedure was run further from perigee, where Earth's magnetic field is weaker.

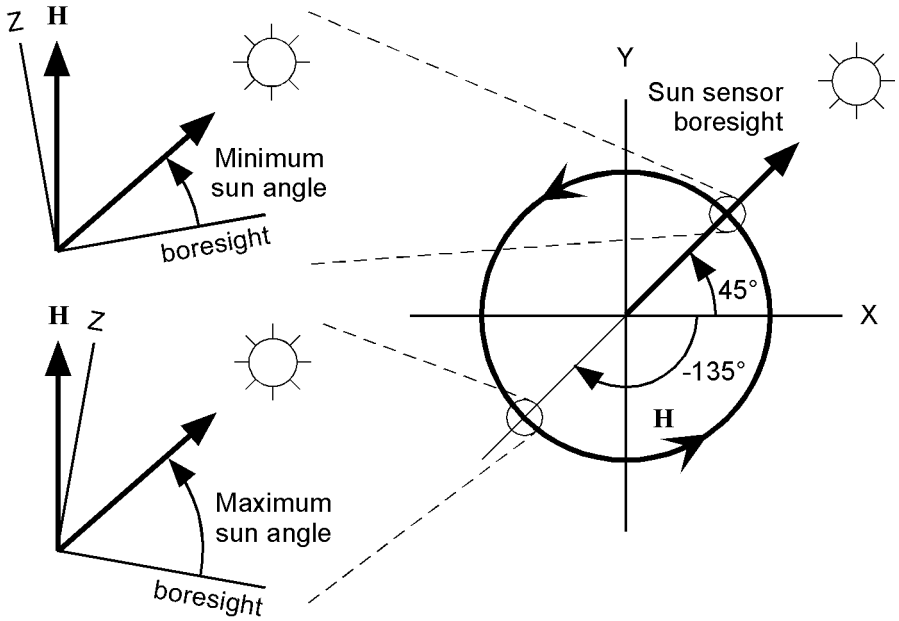

Figure 12. Sun angle variation due to nutation

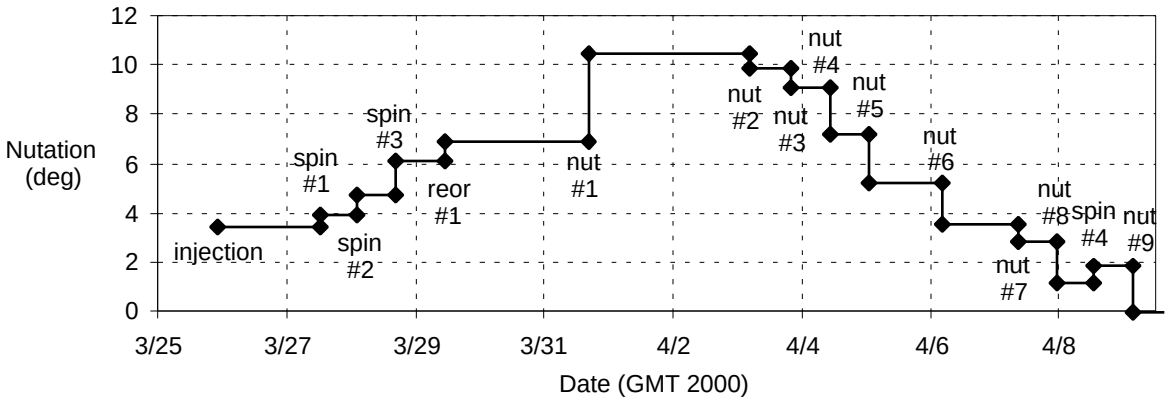

Figure 13. Nutation history during first 15 days of IMAGE flight operations (spin = spin rate change maneuver, reor = spin axis reorientation maneuver, nut = magnetic damper nutation damping maneuver)

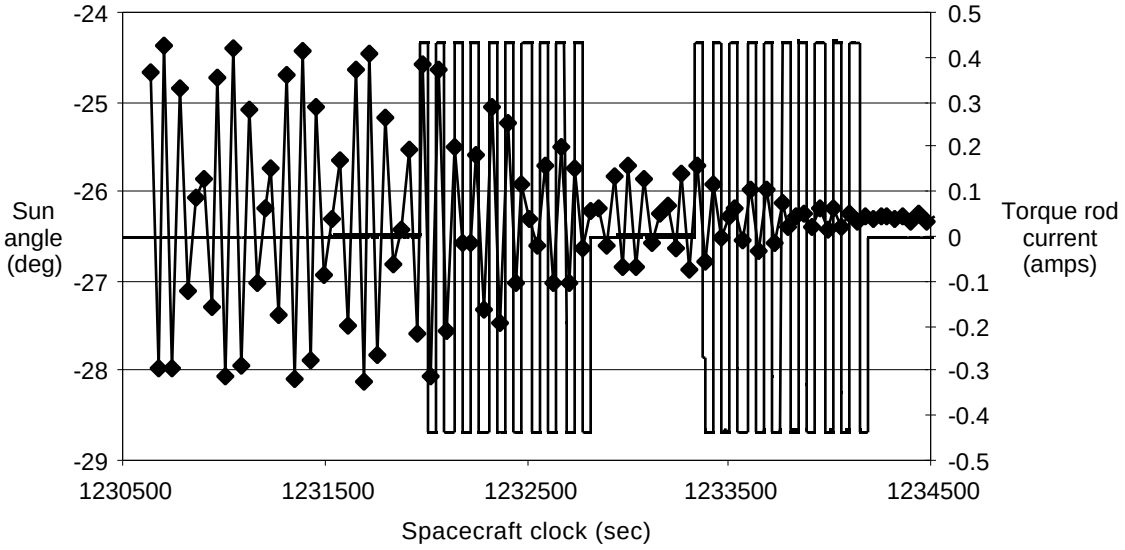

Figure 14. Sun angle and magnetic torque rod current during nutation damping

The procedure was repeated on seven additional orbits between April 3 and April 9. This reduced nutation to 0.04º. Figure 14 shows the torque rod current and measured sun angles on the last of these orbits. On this particular orbit the procedure was executed twice, reducing nutation from 1.93º to 0.59º on the first cycle and to 0.04º on the second. With the nutation problem successfully resolved, normal mission operations were resumed.

CONCLUSIONS

Analysis of IMAGE flight data confirmed the hypothesis that surface tension lockup prevented nutation damping during early portions of the IMAGE mission. This behavior makes it clear that partially filled ring dampers should not be used at spin rates for which the centrifugal Bond number is less than 1. The successful resolution of IMAGE's nutation problem confirms yet again the value of being able to manually command control actuators in real time.

REFERENCES

1. Herzl, G., "Introduction to Passive Nutation Dampers", Proceedings of the NASA Goddard Space Flight Center 5th Aerospace Mechanisms Symposium, 1971, pp. 73-81.

2. Carrier, G., and Miles, J., "On the Annular Damper for a Freely Precessing Gyroscope", *Journal of Applied Mechanics*, June 1960, 237-240.

3. Miles, J., "On the Annular Damper for a Freely Precessing Gyroscope - II", *Journal of Applied Mechanics*, June 1963, 189-192.

4. Cartwright, W., Massingill, E., and Trueblood , R., "Circular Constraint Nutation Damper", *AIAA Journal*, Vol. 1, No. 6, 1963, pp. 1375-1380.

5. Alfriend, K., "Analysis of the Partially Filled Viscous Ring Damper", NASA-CR-139011, 1973.

6. Alfriend, K., "Partially Filled Viscous Ring Nutation Damper", *Journal of Spacecraft and Rockets*, Vol. 11, No. 7, 1974, pp. 456-462.

7. Ancher, L., van den Brink, H., and Pouw, A., "Asymmetric Oscillation of a Passive Nutation Damper", *Proceedings of the CNES-ESA Conference on Attitude Control of Space Vehicles*, ESA SP-129, 1977, pp. 179-183.

8. Schmieder, L., "Investigations of Annular Dampers for Spinning Space Vehicles", *Proceedings of the CNES-ESA Conference on Attitude Control of Space Vehicles*, Paper SP-129, 1977, pp. 185-192.

9. Alfriend, K., and Spencer, T., "Comparison of Filled and Partly Filled Nutation Dampers," AAS/AIAA Astrodynamics Conference, Paper AAS 81-141, 1981.

10. Hinada, M., and Inatani, Y., "Liquid Behavior in Passive Nutation Dampers for Spin Stabilized Satellites", *Transactions of the Japan Society for Aeronautical and Space Sciences*, Vol. 27, No. 78, 1985, pp. 217-227.

11. King, G., and Woolley, R., "Modeling, Tuning, and Effectiveness of Partially-Filled Ring Nutation Dampers", AAS Rocky Mountain Guidance and Control Conference, Paper AAS 85-054, 1985.

12. Chang, C., Chau, C., and Wang, S., "Design of a Viscous Ring Nutation Damper for a Freely Precessing Body", *Journal of Guidance, Control, and Dynamics*, Vol. 14, No. 6, 1991, pp. 1136-114 .

13. Reynolds, R., "Dynamic Modeling of Ring Nutation Dampers", AIAA/AAS Astrodynamics Specialist Conference, Paper AIAA-2000-4533, 2000.

14. Hong, J., "Residual Nutation Angle of Satellites With Viscous Nutation Dampers", 36th International Astronautical Congress, Paper IAF 85-234, 1985.

15. Schwartz, A., and Ellison, A., "The Effect of Surface Contamination on Contact Angles and Surface Potentials", NASA CR-54708, 1966.

APPENDIX - INERTIAL FORCE ON THE LIQUID SLUG

A minimum inertial force is needed to start a liquid slug moving against the restraining effect of surface tension. In this appendix, the inertial force due to nutation is derived. To streamline the analysis, the mathematical model is based on the several simplifying assumptions. Specifically, the spacecraft is assumed to be inertially symmetric, the nutation angle is assumed to be small (less than about 15 deg.), and the liquid mass is assumed to be a negligible fraction of the total vehicle mass. The last assumption implies that the vehicle's center of mass location is unaffected by the location of the liquid slug. The analytical model also assumes an XYZ principal-axis coordinate system, with the Z axis being the spacecraft's nominal spin axis. The vehicle's spin-to-transverse axis inertia ratio is denoted by the symbol γ. If the spin rate is Ω, then its nutation frequency, λ, is given by the following equation:

$$\lambda = (\gamma - 1)\,\Omega \tag{A-1}$$

For small nutation, the angular velocity and angular acceleration vectors are the following functions of time:

$$\omega = [A\cos(\lambda t), A\sin(\lambda t), \Omega]^T \tag{A-2}$$

$$\alpha = A\lambda\,[-\sin(\lambda t), \cos(\lambda t), 0]^T \tag{A-3}$$

The amplitude, A, of the transverse angular rate is related to the nutation angle, Φ, as follows:

$$A = \Phi\,\gamma\,\Omega \tag{A-4}$$

Using parameters defined in Fig. 2, the vector from the vehicle cm to a point on the damper tube centerline is

$$\mathbf{r} = [R_D\cos(\varphi), R_D\sin(\varphi), h]^T \tag{A-5}$$

where φ is an angular position measured from the X axis as shown in Figure A-1. The unit vector tangent to the tube centerline at angular position φ is given by

$$\mathbf{u} = [-\sin(\varphi), \cos(\varphi), 0]^T \tag{A-6}$$

If the liquid slug is to remain stationary relative to the tube, it must accelerate relative to inertial space. At angular position φ, this inertial acceleration is

$$\mathbf{a} = (\alpha \times \mathbf{r}) + \omega \times (\omega \times \mathbf{r}) \tag{A-7}$$

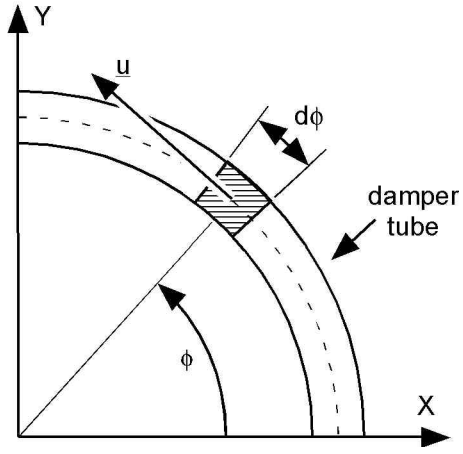

Figure A-1. Differential element of the liquid slug

The component of this acceleration that is tangent to the tube centerline is the portion that must be applied by surface tension if the liquid is to be held in place. This component is give by

$$a_T = \mathbf{u} \bullet \mathbf{a} \tag{A-8}$$

The force necessary to impart this acceleration component to a differential slug element of angular length $d\varphi$ is

$$dF_T = a_T\,\rho\,(\pi R_T^2)\,R_D\,d\varphi \tag{A-9}$$

The total force on the liquid slug is simply the integral of Eqn. A-9. Because the slug is a liquid, this

integration is valid even though the path is curved. Our concern is the net reaction force on the surface tension "membranes" at the ends of the slug, and this force results from a cumulative pressure differential between the two ends. (Note that the reaction force is the negative of the integral of Eqn. A-9.) For a stationary slug, the inertial force is sinusoidal at the nutation frequency. Our concern is to find the amplitude of that sinusoid.

For simplicity, the remaining steps of the analysis will focus on the conditions that exist at time zero. Specifically, the liquid slug will be located at an angular position that yields the maximum value for the reaction force on the surface tension membranes at $t = 0$, and an expression for that value will be derived. This assumption involves no loss of generality. Since the vehicle is assumed to be symmetric, the maximum value of the reaction force is independent of the slug's location. The maximum value simply occurs at a time other than zero at different angular locations.

At time zero, the maximum possible reaction force on the surface tension "membranes" occurs when the liquid slug is centered on $\varphi = \pi/2$. With a slug half angle of β (Fig. 2), the peak reaction force on the slug due to nutation is

$$F_N = -\int_{(\pi/2)-\beta}^{(\pi/2)+\beta} [a_T \rho(\pi R_T^2) R_D]\, d\varphi \tag{A-10}$$

After appropriate substitutions and integration, we have the following result:

$$F_N = 2\pi h \gamma^2 \rho \Phi \Omega^2 \sin(\beta) R_D R_T^2 \tag{A-11}$$

As indicated above, if the spacecraft is not inertially symmetric then F_N will be a function of the slug's position within the tube. At some locations, the force will be greater than indicated in Eqn. A-11 and at other locations it will be less. As nutation damps, the slug is likely to settle into a location that minimizes F_N. Hence, a slug release angle that is calculated based on Eqn. A-11 is likely to be an underestimate if the vehicle is asymmetric.